31 Cassini Corneal Topographer

Joris Snellenburg, Maarten Huijbregtse, Benhur Ortiz-Jaramillo, Masmei Ginting, and Ernst Serfontein

Introduction

Cassini provides cataract surgeons with an accurate and detailed description of the cornea, helping them to improve their surgical outcomes, reducing the number of postoperative surprises, and cutting the number of patients requiring follow-up corrective laser treatments. Cassini addresses the most important sources of corneal errors in cataract surgery, using a unique reflection-based technology, with color and infrared LED illumination (Fig. 31.1).

Over the past two decades, surgeons have been able to improve the outcomes of cataract procedures considerably due to more sophisticated IOL power formulas, as well as more advanced optical biometers. Despite these advancements, even today, the accuracy of the refractive predictions is still far from perfect even for virgin corneas [1]. In an endeavor to further reduce postoperative errors, reliable preoperative corneal measurements are essential, particularly of the first refractive layer: the tear film. As the cornea accounts for about two-thirds of the total dioptric power of the eye, small variations in the measured corneal shape can have a large effect on the recommended power of an IOL [2].

Fig. 31.1 The Cassini Device

Cassini uses reflection-based technology to measure the shape and state of the tear film. The quality of the tear film layer can be assessed by analyzing the appearance of the reflected LEDs: sharp reflections indicate a smooth tear film layer, while distorted reflections indicate a disrupted tear film layer.

J. Snellenburg (✉) · M. Huijbregtse · B. Ortiz-Jaramillo · M. Ginting · E. Serfontein
Cassini Technologies B.V., The Hague, The Netherlands
e-mail: j.snellenburg@cassini-technologies.com; m.huijbregtse@cassini-technologies.com; b.ortiz-jaramillo@cassini-technologies.com; n.ginting@cassini-technologies.com; e.serfontein@cassini-technologies.com

J. Aramberri et al. (eds.), *Intraocular Lens Calculations*, Essentials in Ophthalmology,
https://doi.org/10.1007/978-3-031-50666-6_31

In addition to assessing the quality of the tear film, it is important to consider the *entire* shape of the surface to judge the accuracy of the displayed K-readings. Unlike the K-readings may suggest, the shape of the cornea is far more intricate than the toric model described by these two radii of curvatures. Irregular features and the aspheric shape of the cornea can have a large impact on the K-readings and limit their validity as an approximation of the entire corneal shape. Cassini measures the entire shape of the anterior surface of the cornea, including the peripheral zone, using hundreds of LEDs. A quick assessment of the topographic maps will highlight irregular features such as cones and irregular astigmatism. If present, surgeons should carefully assess the reliability of the displayed K-readings before using them to calculate the power of an IOL.

Cassini is a pioneer in measuring the shape of the posterior corneal surface using LED technology. The anterior and posterior corneal data can be used together to determine the corneal ratio, helping surgeons by indicating the risk of a myopic or hyperopic shift. Also, planning for toric IOLs can be improved using total corneal astigmatism.

Altogether, the Cassini corneal shape analyzer helps surgeons to make the right decisions for their patients. Cassini connects to the latest surgical devices, exporting reliable preoperative data into surgery and allowing surgeons to maintain high accuracy while speeding up their procedures.

Cassini's mission is to offer highly accurate, personalized data for each patient undergoing cataract surgery to enable the best possible outcomes, even for those patients with challenging corneas.

Cassini Basic Principle

Cassini employs a dual modality system for imaging of the human eye in both the visible and infrared spectrum. A multitude of colored and infrared LEDs serve as illumination sources, as well as data points for its topography modules that measure the anterior and posterior surfaces of the cornea.

The anterior surface is measured by projecting the signature pattern of color LEDs onto the eye. The emitted light reflects off the convex mirror constituted by the tear film of the anterior corneal surface, toward the RGB camera inside the Cassini device (Fig. 31.2). The shape of the cornea is modeled as a linear combination of Zernike

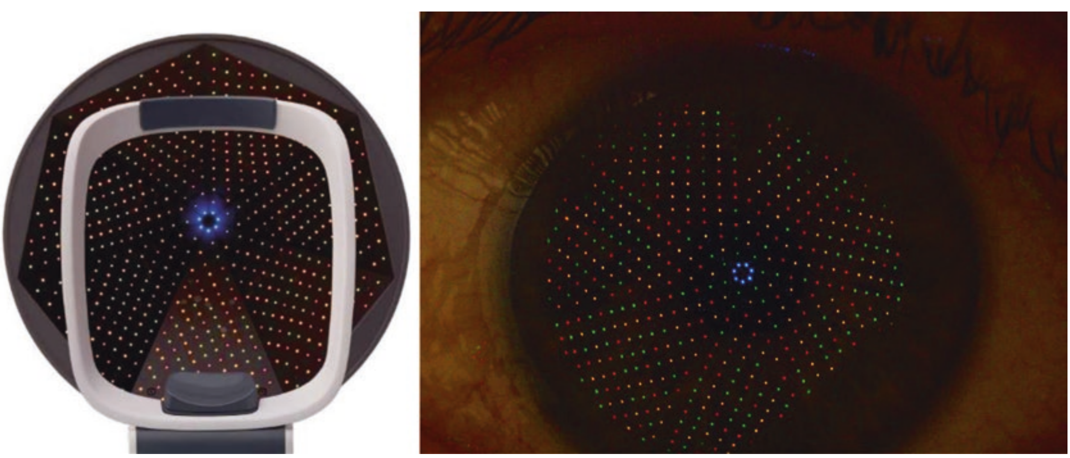

Fig. 31.2 Cassini's signature, color-coded LED pattern (left) and its reflection off an eye as imaged by the RGB camera (right)

polynomials, where the polynomial coefficients are iteratively updated using ray tracing until the differences between the angles of incidence and the angles of reflection are minimized in a least squares sense [3]. Color coding of the LED pattern ensures a direct relationship between each image point and a corresponding source point. Skew ray errors are thus avoided and, in combination with the sampling density, this allows for highly detailed and accurate surface measurements—especially considering the axis of astigmatism and higher-order aberrations [4].

A small fraction of the source light will not directly reflect off the anterior surface, but traverse through the cornea and reflect off the posterior surface instead—an effect that is enhanced in the infrared spectrum and utilized by Cassini to determine the global posterior surface shape with its infrared imaging system. Source light emitted from multiple infrared LEDs is captured by an infrared camera after reflecting off the corneal surfaces (Fig. 31.3). Ray tracing and an extended corneal model—including the anterior and posterior surface separated by a corneal thickness—are combined to determine the posterior toric shape that best fits the image data in a least squares sense. The posterior measurement captures the relevant information to investigate the effects of the posterior surface on the total corneal power and astigmatism.

In addition to the topographic capabilities, Cassini's imaging system can be used to derive other ocular metrics like tear film dynamics, horizontal visible iris diameter, and pupil sizes under various lighting conditions.

Acquired data is presented in a concise, yet complete overview in the Cassini software GUI (Fig. 31.4). Customizable settings for, e.g., color keys, units, and overlays allow for data interpretation in a personalized manner. Cassini's printing suite transfers the data in a similarly concise format to a variety of reports tailored to the surgical plan under consideration—whether pertaining to astigmatism correction, multifocal IOL, FLACS, or any combination thereof.

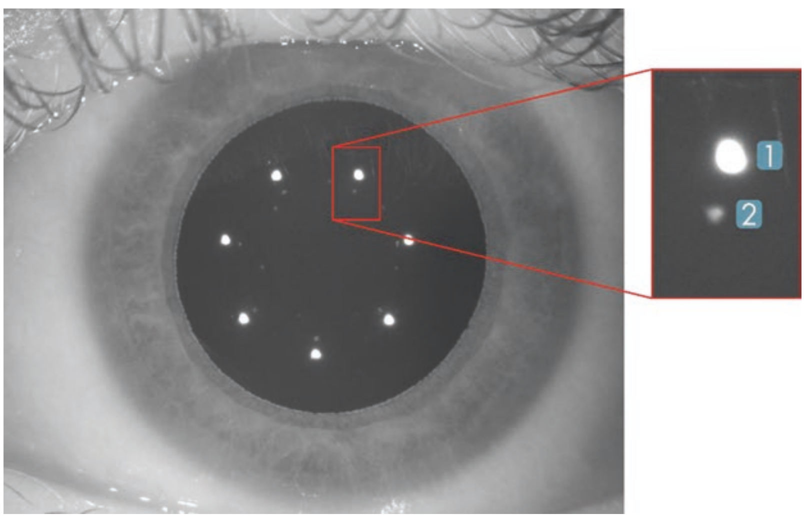

Fig. 31.3 Infrared image of an eye, showing the infrared LED reflections from the anterior surface (1) and posterior surface (2)

Fig. 31.4 Cassini's highly customizable layout featuring, e.g., color scales, custom ordering in the 6-up view, opening in a detailed 1-up view, printing reports, or writing notes

Surgical Planning with Cassini

Monofocal IOLs

All IOL power formulas, even the latest and most sophisticated models, strongly rely on the flat and steep K-readings [5]. These two K-readings summarize the power distribution of the entire anterior corneal surface into a simplistic toric representation. It is therefore important that the K-readings plugged into the IOL power calculators are a reliable representation of the true anterior surface of the cornea, which is typically far more complex. Care must be taken especially for post-refractive corneas and poor tear film layers. To avoid postoperative surprises, Cassini users are advised to review the preoperative data thoroughly. Deleting and repeating a bad measurement before surgery is always preferable to avoid postoperative surprises, conducting refractive touch-ups and disappointed patients [6].

The key aspect to evaluate whether the displayed K-readings are a correct representation of the true shape of the cornea is to look at the overall shape of the cornea. Cassini measures the entire corneal surface and displays its true shape in a series of topographic maps. Astigmatism (bow tie), irregular features (cones) and post-refractive eyes (flattened) have characteristic forms that are easy to identify. Also, in each untreated cornea, the central region is steeper and therefore more powerful than the outer regions of the cornea. Altogether, the magnitude of the K-readings is strongly influenced by the selected corneal region. Care must be taken if devices base their K-readings on just a few measuring points as they might miss relevant information from other regions. Cassini measures the entire corneal surface, revealing important irregularities and helping surgeons to interpret the reliability of the K-readings. Even a quick assessment of these maps will inform the surgeon if the shape is normal or irregular and consequently, if the two K-readings are representative for the entire cornea and can therefore be trusted.

Recent findings by Wang et al. [7] emphasize the significant role of the posterior corneal surface in total corneal refraction, challenging the longstanding assumption that the anterior surface solely dictates corneal power. Traditionally, cataract surgeons relied on a simulated K-reading derived from the anterior surface, based on the presumed constancy of the posterior-to-anterior corneal ratio. However, Wang et al. discovered varying ratios: 0.81 and 0.82 for normal corneas, 0.76 for eyes post-myopic LASIK/PRK, and 0.86 for post-hyperopic LASIK/PRK. These findings highlight the necessity of considering both corneal surfaces in refraction calculations, particularly in eyes that have undergone refractive surgeries, which significantly alter the corneal shape and, consequently, the corneal ratio. Next to modified eyes, studies show the spread in corneal ratio among normal corneas is also significant; to conclude that surgeons cannot use the anterior surface of the eye only to predict the total power of the cornea [8]. Cassini measures both the anterior and posterior surface of the cornea and determines the corneal ratio to indicate whether the simulated corneal readings fit the IOL-power calculations model or not (Fig. 31.5).

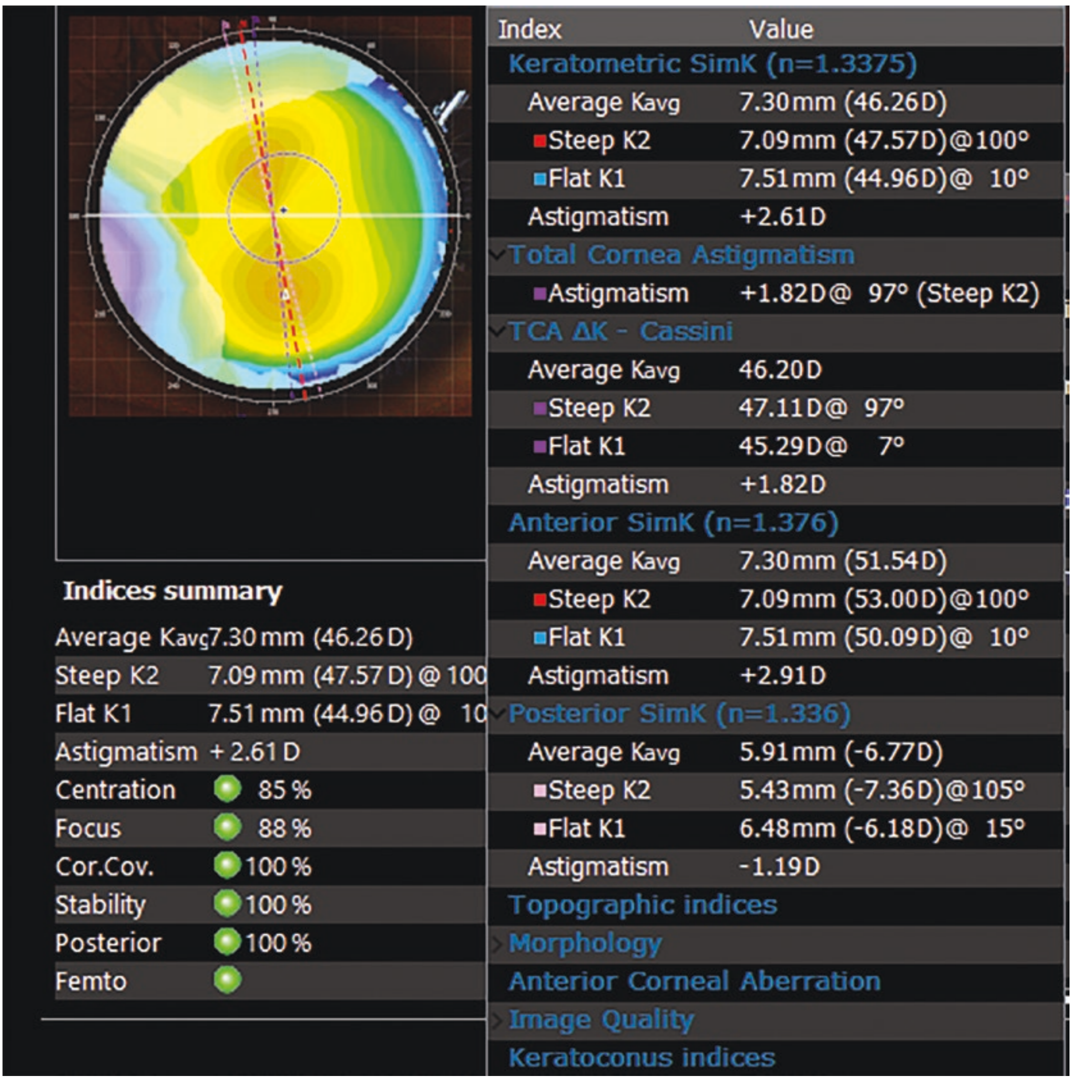

Fig. 31.5 Indices summary with traditional K-readings, examination quality factors and when expanded a host of other properties, including information on the posterior surface and eye morphology

Toric IOLs

Astigmatism is even more sensitive to corneal irregularities. Even nonastigmatic features such as a conic surface will lead to a difference in steep and flat K-readings (astigmatism magnitude), and therefore a false assumption of astigmatism.

The astigmatism-per-zone overlay on Cassini's topographic maps provides insight into the regularity of astigmatism (Fig. 31.6). Regular

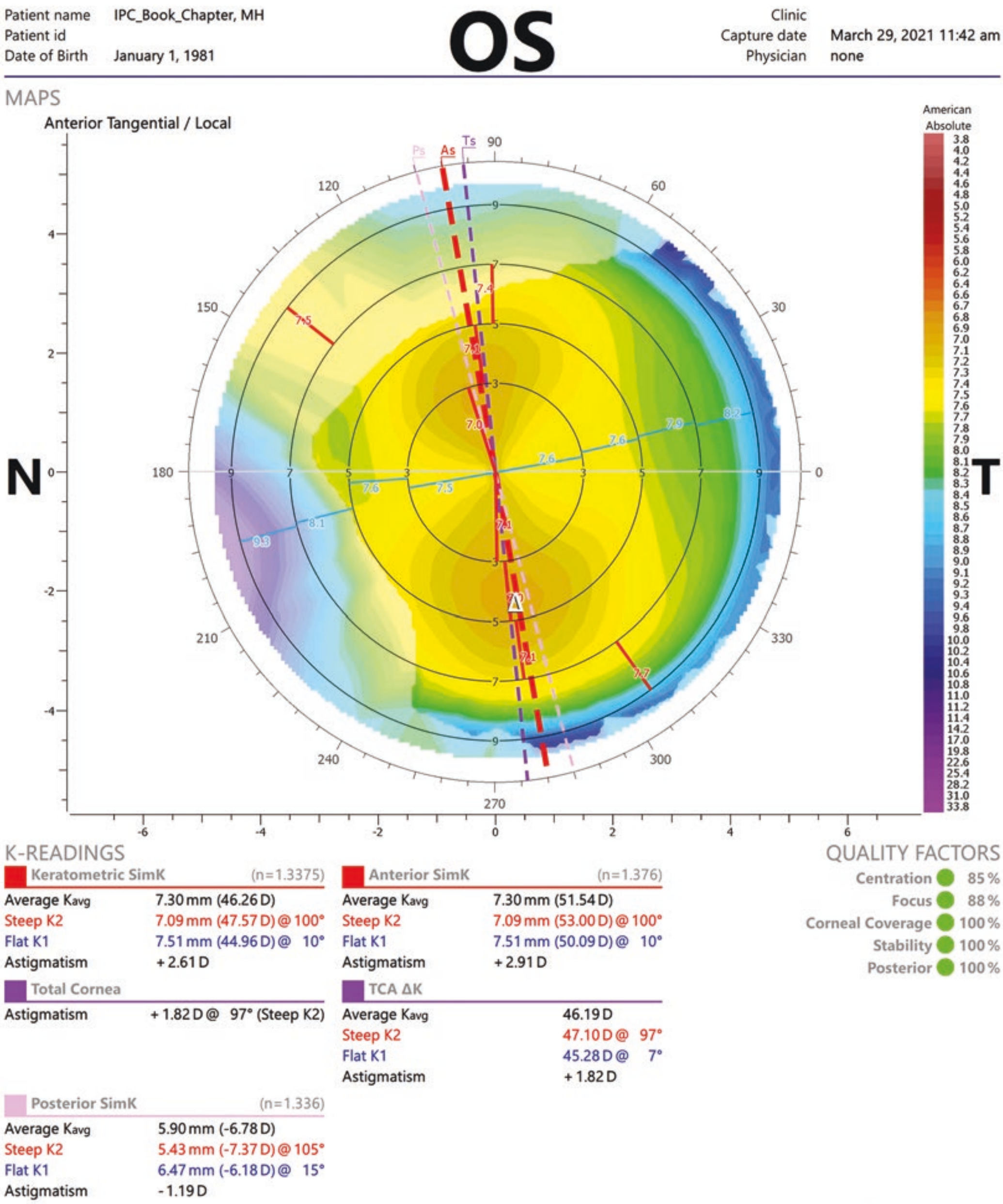

Fig. 31.6 Astigmatism per zone overall featuring a nice symmetric bow tie. Note a significant amount of posterior astigmatism, significantly reducing the total cornea astigmatism resulting in spectacle-free day vision for this healthy volunteer's eye

astigmatism is characterized by a highly symmetric bow tie, whereas irregular astigmatism is characterized by skewed radial axes or an asymmetric bow tie, or both.

In 2012, D. Koch et al. published a study on the contribution of the posterior corneal astigmatism to the total corneal astigmatism [9]. The study played an important role in the awareness of the posterior corneal astigmatism and its prominent effect on corneal astigmatism management. Ignoring the contribution of the posterior corneal astigmatism may lead to an overcorrection in eyes that have with-the-rule astigmatism and undercorrection in eyes that have against-the-rule astigmatism. A few examples are shown in Fig. 31.7. This new insight led to the Baylor Nomogram, which helps surgeons to adjust the power of astigmatism by incorporating population-based averages for the posterior surface [10].

This led to better results on average; however, results are not optimal for all patients due to the weak correlation between the anterior and posterior corneal astigmatism. Cassini directly measures the posterior corneal astigmatism and combines this

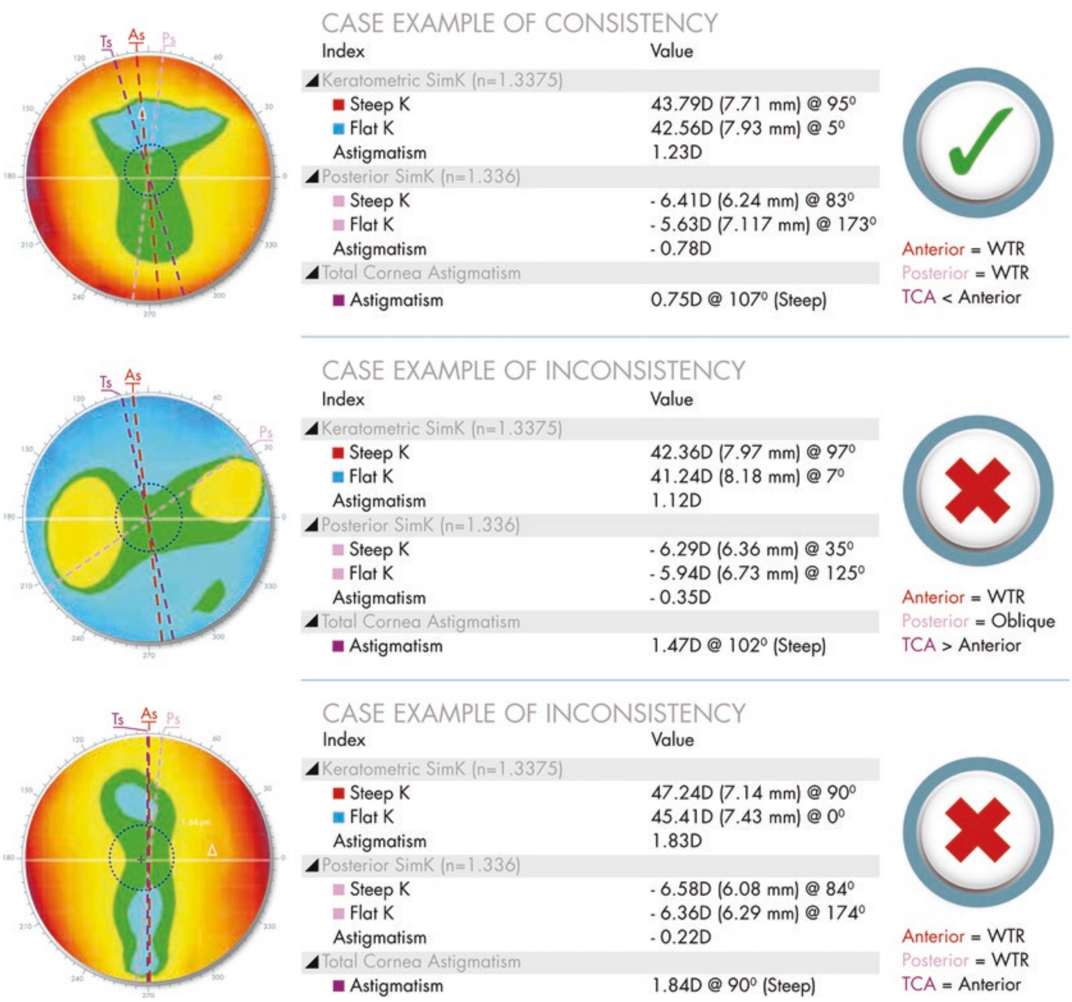

Fig. 31.7 Three example cases where ignoring the posterior contribution may lead to unexpected surprises, specifically when anterior astigmatism is with-the-rule, but posterior is not

with the anterior corneal astigmatism to calculate the total corneal astigmatism (TCA). This does not only lead to the correct power of astigmatism but also to the correct angle of astigmatism. Modern IOL calculators could increase their accuracy by allowing the inclusion of such a parameter within their calculations. Meanwhile, a corneal astigmatism planning report allows surgeons to make use of the information provided by TCA, to be used in conjunction with standard online toric calculators.

Multifocal IOLs

Multifocal intraocular lenses can offer patients spectacle-free vision. Planning multifocal IOLs require detailed preoperative examinations that go beyond the power and astigmatism considerations described above. Irregular features of the cornea such as coma and higher-order aberrations as well as the quality of the tear film become even more important for multifocal IOLs. Loss of contrast and sensitivity associated with multifocal IOLs will become more apparent if the ocular surface is not smooth and the generic shape of the cornea is far from uniform. Cassini calculates the contribution of the higher-order aberrations (HOA) and displays each Zernike component separately. Surgeons can use this information to judge if patients are eligible for multifocal IOLs. Increased higher-order aberrations are common to corneas that have undergone refractive surgery, corneal surgery, poor tear film layers, and conic corneas [11]. Also, the pupil size, shape, and centration significantly influence the quality of vision. Light distribution through the various zones of the multifocal lens depends to a large extent on the size and centration of the pupil. Cassini displays these pupil features under both photopic and mesopic conditions. Incorrect assessment of these parameters may lead to photophobia phenomena like glare and halo. Centration of the multifocal lens in relation to the vertex position of the cornea may also play an important role in the occurrence of unwanted visual effects. The distance between the corneal vertex—or more correctly: "the subject-fixated coaxially sighted corneal light reflex" and pupil center is described by chord mu [12], and historically labeled as Angle KAPPA. The distance between the corneal vertex and the center of the limbus is labeled as Angle Alpha. Cassini reports Angle KAPPA and Angle Alpha for both the photopic and mesopic pupil conditions (Fig. 31.8).

FLACS

Femtosecond laser-assisted cataract surgery (FLACS) can be used to assist the surgeon in managing patient astigmatism. The structural features of the iris, defined by its muscular configuration, can be used to determine the exact location of the preoperatively measured angle of astigmatism in surgery. The so-called iris registration algorithm uses these fingerprint-like features of the iris to compensate for well-known errors such as cyclotorsion, which can be more than 10 degrees [13]. Manual marking, which often leads to the blurring of ink spots, can be eliminated as well, thereby removing yet another source of error. For the correction of minimal to moderate amounts of astigmatism, FLACS can be used to create arcuate incisions. FLACS can also be used to create radial markings in the cornea or in the capsulorrhexis to identify axis alignment of toric IOLs. Cassini preoperative iris imaging and astigmatism diagnostics allows for increased accuracy in the placement of arcuate incisions and identification marks for toric IOL alignment. Automatic connectivity will reduce manual transcription errors and procedure time.

Cassini currently interfaces with Johnson & Johnson Vision's CATALYS Precision Laser System and the LENSAR Laser System by LENSAR (Fig. 31.9).

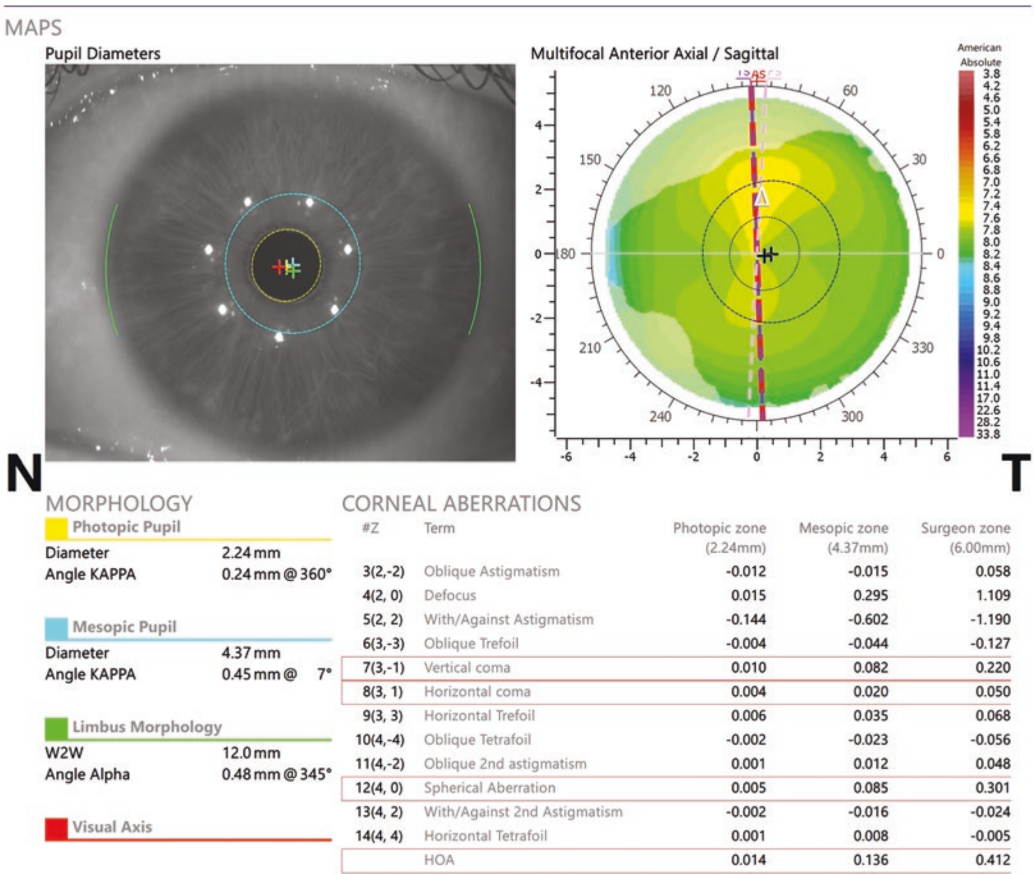

#Z	Term	Photopic zone (2.24mm)	Mesopic zone (4.37mm)	Surgeon zone (6.00mm)
3(2,-2)	Oblique Astigmatism	-0.012	-0.015	0.058
4(2, 0)	Defocus	0.015	0.295	1.109
5(2, 2)	With/Against Astigmatism	-0.144	-0.602	-1.190
6(3,-3)	Oblique Trefoil	-0.004	-0.044	-0.127
7(3,-1)	Vertical coma	0.010	0.082	0.220
8(3, 1)	Horizontal coma	0.004	0.020	0.050
9(3, 3)	Horizontal Trefoil	0.006	0.035	0.068
10(4,-4)	Oblique Tetrafoil	-0.002	-0.023	-0.056
11(4,-2)	Oblique 2nd astigmatism	0.001	0.012	0.048
12(4, 0)	Spherical Aberration	0.005	0.085	0.301
13(4, 2)	With/Against 2nd Astigmatism	-0.002	-0.016	-0.024
14(4, 4)	Horizontal Tetrafoil	0.001	0.008	-0.005
	HOA	0.014	0.136	0.412

Fig. 31.8 Multifocal IOL Planning Report; showcasing a case with a relatively large-angle KAPPA and a less likely candidate for a multifocal IOL

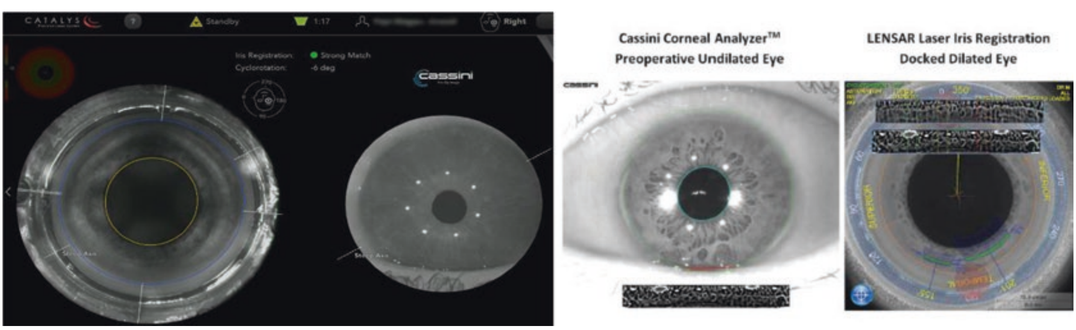

Fig. 31.9 Cassini Connects CATALYS [14] and Cassini Streamlines LENSAR [15]

Ocular Surface Diagnostics (Tear Film)

The ocular surface is covered by a few microns thin liquid film called the tear film. The composition of the tear film is complex and plays an essential role in nourishing and protecting the cornea. The tear film has three distinct layers: (1) the hydrophobic top layer (lipid layer) made of a thin sheet of lipids that reduces surface tension and helps to spread the tears after each blink; (2) the aqueous layer, which is the thickest layer of the tear film and plays, among others, an important role in the oxygenation of the cornea; and (3) the mucous layer, which compensates for corneal unevenness and reduces friction during blinking [16]. Optically, the role of the tear film layer is to form a smooth refractive surface over the uneven corneal surface. At each blink, the tear film layer is being refreshed and goes through a dynamic tear buildup phase to form a tear film layer. The lipid top layer protects the underlying aqueous layer from evaporation. Local rupture in the lipid top layer exposes the aqueous layer directly to air leading to high evaporation rates that potentially produces rupture of the tear film [17]. The time between the formation of the tear film (buildup) and breakup of the tear film depends strongly on the quality of the tear film (mix of lipids and water), the environmental conditions and the pathology of the cornea. The period immediately after the tear buildup phase and before the tear breakup can vary from just a few to more than 20 seconds [18]. Measuring the shape of the first reflective ocular layer should occur in this phase of the inner blink period. Reflection-based technologies, such as Cassini, can use the smoothness of the reflective surface to extract the quality of the tear film layer. Dysfunctional tear glands, wearing of contact lenses and environmental conditions may affect the quality of the tear film. Healthy tear film layers are very even and reflect light like a convex mirror. Tear film layers which tend to breakup, or evaporate quickly, become very uneven, leading to a distortion of the reflective points. From a vision point of view, light crossing these uneven surfaces gets refracted in a similarly uneven way, leading to higher-order aberrations which diminish the image quality at the retina. From a K-reading point of view, instable tear films affect the measured radius of curvature significantly [19]. In this context, Cassini can be used to assess the dynamics (stability) of the tear film by recording the corneal reflection of its projected LED pattern over time. When the surface of the cornea is smooth, each projected color LED appears regular in the image forming a circle-like shape. However, during the inner blink period the tear film changes dynamically: producing localized "dry" regions that leads to distorted shapes of the projected color LEDs in the image (see Fig. 31.10 for comparison). To capture the transition from a circle-like shape to distorted reflection, Cassini processes every frame and monitors the uniformity of every reflected color LED. The distorted LED reflections are marked to indicate potential dry regions.

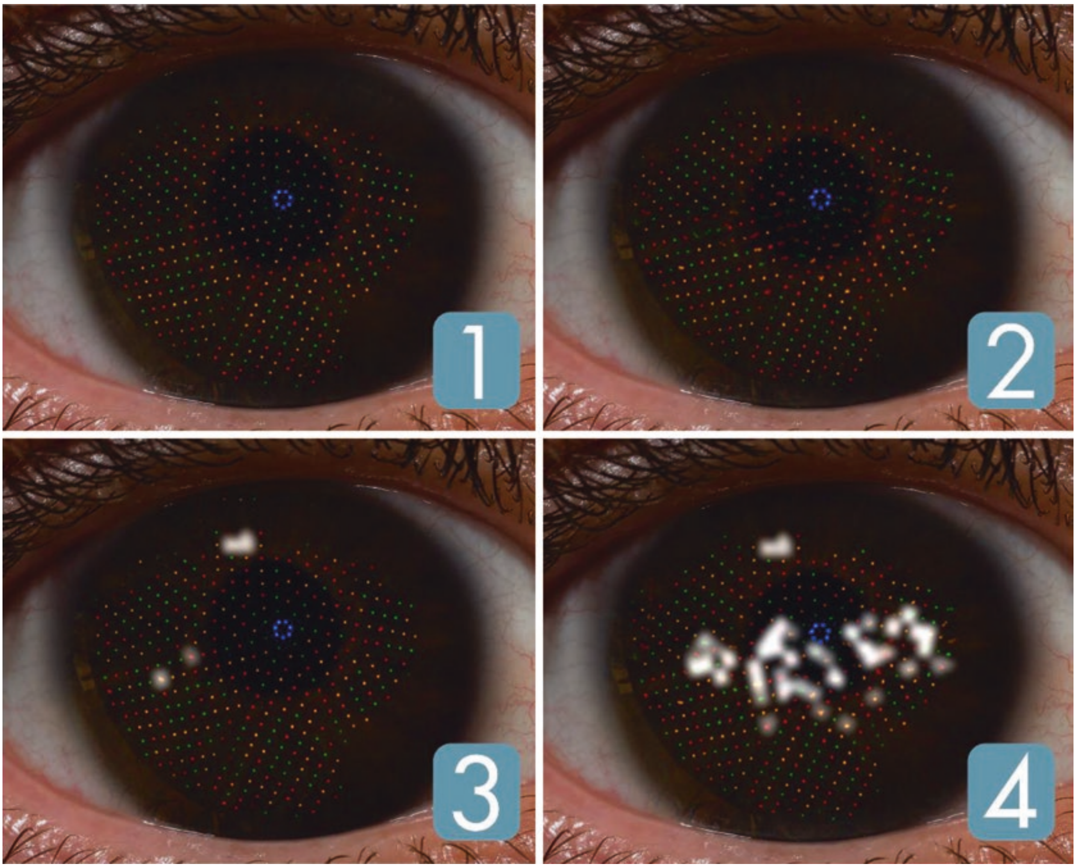

Fig. 31.10 Projected corneal reflection into the colour camera captured with a Cassini device: (1) no degradation of the first Purkinje image and (2) first Purkinje image degraded. (3, 4) Lower 2 images are processed images where the degradation is highlighted in white

Conclusion

Reflection-based corneal topography is not something new, but Cassini's distinct and unique measuring principle sets it apart from other technologies. With close to 700 multicolor LEDs, as well as the ability to measure the posterior surface of the cornea by means of second Purkinje reflections, Cassini has taken the "proven" point-measurement system to a new level (Fig. 31.11). It is therefore a clearly differentiating platform with its primary application in the field of cataract surgery.

CASSINI
SPECIFICATIONS

Submicron accuracy with up to 700 ambient multicolor LEDs combined with 2nd Purkinje raytracing technology

Anterior axis repeatability within 3 degrees [8]

Keratometric data display of Steep, Flat and Average in Diopters and millimeters for anterior, posterior and Total Corneal Astigmatism (TCA)

Topographic indices: Shape factor (E), eccentricity (e), Asphericity (Q) and form factor (p)

Topography mapping: Axial, Refractive, Tangential and Elevation

Multiple color keys for topography map customization

Keratoconus screening indices: Surface Asymmetry Index (SAI) and Surface Regularity Index (SRI)

Corneal aberrations with individual Zernike terms and total HOA parameter display

Multifocal IOL suitability module with White-to-White, Pupillometry, Angle Alpha and Angle KAPPA

External Ocular Photography

Seamless ocular surface screening and visualization module

Automated and manual capturing with joystick positioning on visual axis

Accuracy verification with Quality Factors

Incorporated Iris Registration for Femtosecond Laser Assisted Cataract Surgery (FLACS)

Encrypted patient management with various clinical report export options: DICOM, USB, Wi-Fi, PDF, JPG and PNG

Fig. 31.11 Cassini specifications

References

1. Koch DD, Hill W, Abulafia A, Wang L. Pursuing perfection in intraocular lens calculations: I. Logical approach for classifying IOL calculation formulas. J Cataract Refract Surg. 2017;43(6):717–8.
2. Larkin H. Bright path ahead: Examining six requirements for reducing errors and eliminating 'refractive surprise'. Eurotimes Stories; 2017. https://www.eurotimes.org/refractions/
3. Snellenburg JJ, Braaf B, Hermans EA, van der Heijde RGL, Sicam VADP. Forward ray tracing for image projection prediction and surface reconstruction in the evaluation of corneal topography systems. Opt Express. 2010;18(18):19324–38.
4. Klein SA. Corneal topography reconstruction algorithm that avoids the skew ray ambiguity and the skew ray error. Optom Vis Sci. 1997;74(11):945–62.
5. Savini G, Taroni L, Hoffer KJ. Recent developments in intraocular lens power calculation methods - update 2020. Ann Transl Med. 2020 Jul;8(22):1–9.
6. Hill WE, Abulafia A, Wang L, Koch DD. Pursuing perfection in intraocular lens calculations. II. Measuring foibles: Measurement errors, validation criteria, IOL constants, and lane length. J Cataract Refract Surg. 2017;43(7):869–70.
7. Li Wang, Ashraf M. Mahmoud, Betty Lise Anderson, Douglas D. Koch, Cynthia J. Roberts; Total Corneal Power Estimation: Ray Tracing Method versus Gaussian Optics Formula. Invest. Ophthalmol. Vis. Sci. 2011;52(3):1716–22.
8. Haigis W, Hoffer KJ, Holladay JT, Olsen T. The Creator's Forum: IOL power calculations for postrefractive surgery eyes. CRSTEurope 2012 MayE.
9. Koch DD, Ali SF, Weikert MP, Shirayama M, Jenkins R, Wang L. Contribution of posterior corneal astigmatism to total corneal astigmatism. J Cataract Refract Surg. 2012;38(12):2080–7.
10. Koch DD, Jenkins RB, Weikert MP, Yeu E, Wang L. Correcting astigmatism with toric intraocular lenses: effect of posterior corneal astigmatism. J Cataract Refract Surg. 2013;39(12):1803–9.
11. Taskov G, Taskov T. Higher order aberrations (HOA) changes after Femto-LASIK in topography and wavefrontguided treatments. Folia Med. 2020;62:331.
12. Chang DH, Waring GO. The subject-fixated coaxially sighted corneal light reflex: a clinical marker for centration of refractive treatments and devices. Am J Ophthalmol. 2014 Nov;158(5):863–74.
13. Febbraro JL, Koch DD, Khan HN, Saad A, Gatinel D. Detection of static cyclotorsion and compensation for dynamic cyclotorsion in laser in situ keratomileusis. J Cataract Refract Surg. 2010;36(10):1718–23.
14. Internal Image Collection. 2021. Collected by Trey Bishop, MD. Bishop Eye Center, Hilton Head, South Carolina.
15. Cataract & Refractive Surgery Today: Intelligent Integration for Optimal Outcomes, Cataract Surgery Feature Stories. July 2015. Mark Packer, MD, CPI.
16. Anga M, Baskaran M, Werkmeister RM, Chua J, Schmidl D, dos Santos VA, Garhöfer G, Mehta JS, Schmetterer L. Anterior segment optical coherence tomography. Prog Retin Eye Res. 2018;66:132–56.
17. King-Smith PE, Fink BA, Nichols JJ, Nichols KK, Hill RM. Interferometric imaging of the full thickness of the precorneal tear film. J Opt Soc Am A Opt Image Sci Vis. 2006;23(9):2097–104.
18. Willcox M, Argüeso P, Georgiev HJ, Laurie G, Millar T, Papas E, Rolland J, Schmidt T, Stahl U, Suarez T, Subbaraman L, Uçakhan O, Jones L. TFOS DEWS II tear film report. Ocul Surf. 2017;15:369–406.
19. Doğan A, Gürdal C, Köylü M. Does dry eye affect repeatability of corneal topography measurements? Turk J Ophthalmol. 2017;48:57–60.